AIAA JOURNAL
Vol. 41, No. 3, March 2003

Nonequilibrium Radio Frequency Discharge Plasma Effect on Conical Shock Wave: $M = 2.5$ Flow

Peter Palm,* Rodney Meyer,† Elke Plönjes,* J. William Rich,‡ and Igor V. Adamovich§
The Ohio State University, Columbus, Ohio 43210-1107

An experimental study of shock modification in an $M = 2.5$ supersonic flow of nonequilibrium plasma over a cone is discussed. The experiments are conducted in a nonequilibrium plasma supersonic wind tunnel. Recent experiments at the Ohio State University using a supersonic plasma flow over a quasi-two-dimensional wedge showed that an oblique shock can be considerably weakened by a transverse rf discharge plasma. The previously observed shock weakening, however, has been found consistent with a temperature rise in the boundary layers heated by the discharge. In the present study, the boundary-layer effects on the shock wave are reduced by placing an entire cone model into a supersonic inviscid core flow. The electron density in the supersonic plasma flow in the test section is measured using microwave attenuation. The ionization fraction in the discharge is in the same range as in the previous plasma shock experiments, up to $n_e/N = (1.2\text{–}3.0) \times 10^{-7}$. The results do not show any detectable shock weakening by the plasma. This strongly suggests that the previously observed shock weakening and dispersion in nonequilibrium plasmas are entirely due to thermal effects.

I. Introduction

SHOCK wave propagation in weakly ionized glow discharge plasmas (with ionization fractions of $n_e/N \sim 10^{-8}$–10^{-6}) has been extensively studied over the past 15 years, both in Russia[1–11] and in the United States.[12–19] A number of anomalous effects, such as shock acceleration, weakening, and dispersion have been reported. These effects have been observed in discharges in various gases (air, N_2, Ar) at pressures up to $P = 30$ torr, and for Mach numbers $M = 1.5$–4.5. They have also been reported to persist for a long time after the discharge is off (up to ~1 ms). These results led to a suggestion that the anomalous shock wave behavior in nonequilibrium plasmas is primarily due to the effect of the speed of sound and the flowfield modification by the charged species, for example, ion-acoustic wave,[20] or by the metastable species[21–23] present in the plasma.

Recent experimental and modeling results suggest that these effects can be explained by nonuniform gas heating in the discharge. Indeed, pulsed glow discharge/shock tube experiments[16] demonstrate that shock weakening and dispersion in glow discharge plasmas are no longer observed when the gas temperature gradients are reduced to a minimum. In addition, several computational fluid dynamics models predict acceleration, weakening, and dispersion of the shock wave propagating across axial and radial temperature gradients (without plasmas),[24–26] fairly consistent with the experiments. Finally, analysis of possible plasma-related mechanisms of the flowfield modification (ion-acoustic waves, energy storage by metastable species, etc.) shows that both these phenomena have a negligible effect on the shock wave propagation.[27] This occurs for two basic reasons: 1) The ionization fraction in these plasmas is far too low for the charged species, perturbed by the shock, to produce significant coupling with the neutral species flowfield. 2) The amount of energy stored in the metastables is too low, or the metastable relaxation rate is too slow to affect the energy balance in the shock.

Recently, experimental studies of shock modification have been conducted at the Ohio State University using a nonequilibrium plasma supersonic wind tunnel.[17,18] In this experiment, an oblique shock attached to a wedge located in a supersonic flow of a cold, nonequilibrium N_2–He plasma was monitored using high-pressure plasma flow visualization. The plasma was produced by an aerodynamically stabilized diffuse dc glow discharge[17] sustained in the tunnel plenum and by a transverse rf discharge[18] sustained in the supersonic test section. The advantage of this experiment is that a stationary shock is observed in a steady-state plasma flow with well-characterized parameters. In addition, in this experiment the ionization is sustained in a cold supersonic flow without producing considerable gas heating. In other words, the thermal and ionization effects are uncoupled. Such an experiment can determine whether ionization contributed to acceleration, weakening, and dispersion of shock waves in glow discharge plasmas observed in previous experiments[1,2,12,13] or whether these effects are entirely due to radial and axial temperature gradients present in the plasma.

Previous measurements[18] showed considerable oblique shock angle increase with the rf discharge turned on, that is, shock weakening. With the rf discharge on, the shock angle increased from its baseline value of $\alpha = 99$ deg to $\alpha' = 113$ deg, which corresponds to an apparent Mach number reduction from $M = 2.06$ to 1.88. However, both the observed shock weakening and its subsequent recovery after the rf discharge was turned off occurred on a long timescale, over a few seconds. For comparison, the supersonic flow residence time in the test section was of the order of 50 μs. In addition, the observed Mach number reduction was found to be consistent with the temperature increase in the boundary layers on the test section walls, adjacent to the transverse rf discharge electrodes. These observations suggest that the observed shock weakening is likely to be due to thermal effects, in particular, oblique shock interaction with the heated boundary layers.

The present paper discusses the results of a follow-on experimental study where the boundary-layer effects on the shock are reduced. The main objective of this work is to determine whether the shock weakening by plasmas reported in previous studies at the Ohio State University and elsewhere is indeed due to thermal effects.

II. Experimental Facility

The facility used in the present study is a modification of a recently developed, small-scale, steady-state nonequilibrium plasma wind tunnel.[17,18] The design and operation of the wind tunnel has been described in greater detail in Refs. 17 and 18. Briefly, the supersonic flow of nonequilibrium plasma in the wind tunnel is produced by

Received 29 August 2001; revision received 2 July 2002; accepted for publication 8 October 2002.

*Postdoctoral Researcher, Nonequilibrium Thermodynamics Laboratory, Department of Mechanical Engineering.

†Graduate Research Assistant, Nonequilibrium Thermodynamics Laboratory, Department of Mechanical Engineering.

‡Ralph W. Kurtz Professor of Mechanical Engineering, Nonequilibrium Thermodynamics Laboratory, Department of Mechanical Engineering. Associate Fellow AIAA.

§Associate Professor, Nonequilibrium Thermodynamics Laboratory, Department of Mechanical Engineering. Associate Fellow AIAA.

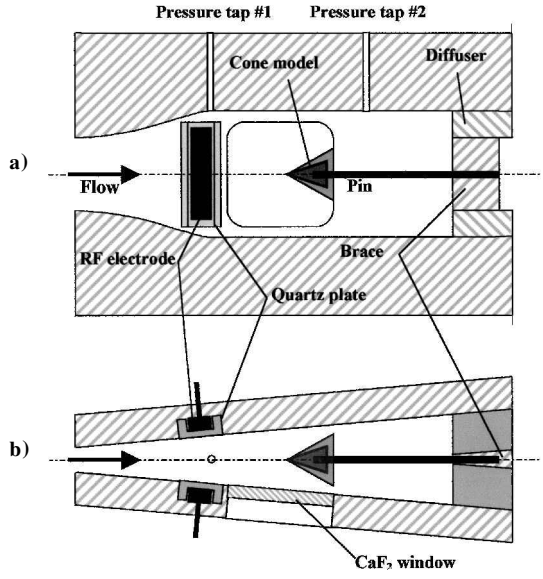

Fig. 1 Schematic of the supersonic rf discharge/test section: a) side view and b) top view.

an aerodynamically stabilized diffuse dc glow discharge[17] sustained in the tunnel plenum and by a transverse rf discharge[18] sustained in the supersonic test section. Both discharges can be sustained at quite high plenum and test section pressures, up to $P_0 = \frac{2}{3}$ atm and $P_{\text{test}} = 0.1$ atm, respectively, in nitrogen and air. Operation at relatively high plenum pressures creates a supersonic flow of reasonable quality (~75% inviscid core), in the test section of the tunnel.[17] At $M = 2$, run durations of at least a few minutes are attained.[18] This is not an arc-heated tunnel. Although the electrical power into the discharges can be rather high, up to 500-W dc and 300-W rf in pure N_2, up to about 90% of the input power goes into the vibrational and electronic energy modes of nitrogen.[28] In contrast to an electric arc, very little of the power goes directly to gas heating. Therefore, conditions of the gases in the test section exhibit the extreme thermal disequilibrium of the positive column of a glow discharge. The translational/rotational mode temperature is low (~100–200 K), the energy in the vibrational mode is high (0.1–0.2 eV per diatomic molecule), the electron density is $n_e \sim 10^{11}$ cm^{-3}, and the average electron energy is in the 1.0 eV range.

Downstream of the plenum/dc discharge section is a 9-cm-long, rectangular cross section supersonic nozzle, shown in Fig. 1. The nozzle is made of transparent acrylic plastic, with a CaF_2 window, which provides optical access to the test section, both in the visible and in the infrared. Fabrication and use of a range of nozzles with varying expansion ratios and test section lengths is straightforward and rapid. The nozzle is connected, through a simple step diffuser, to a ballast tank pumped by a several-hundred-cubic-feet-per-minute vacuum pump. To reduce the effect of the side wall boundary layers on the supersonic inviscid core flow, the side walls of the nozzle are diverging at a constant angle of 5.5 deg. This also allows accommodation of a small plastic cone model in the test section. The nozzle throat and exit dimensions are 17 × 3 mm and 29 × 20 mm, respectively. During the wind-tunnel operation, static pressure in the test section is monitored using two pressure taps in the top nozzle wall, one between the rf electrodes and the other approximately halfway between the electrodes and the diffuser (Fig. 1). The diameter of the pressure taps is about 0.2 mm.

In the present experiment, the dc discharge in the nozzle plenum is used only for supersonic plasma flow visualization.[17,18] Previous experiments[17] showed that turning the dc discharge on and off did not produce a detectable effect on the shock angle. On the other hand, the rf discharge is primarily used to produce ionization in the supersonic test section. The rf discharge is sustained between 17-mm-long, 4-mm-wide strip copper electrodes embedded in the nozzle side walls, as shown in Fig. 1. Both rf electrodes are placed inside the C-shaped rectangular quartz channels, as shown in Fig. 1, to prevent secondary electron emission, which would result in the discharge collapse into an arc. The thickness of the quartz layers between the electrodes and the flow is 1 mm. The electrodes do not extend wall to wall (Fig. 1) because this would produce considerable discharge and temperature nonuniformity in the boundary layers because of the long flow residence time there. The rf voltage was applied to the electrodes using an ENI 13.56-MHz, 600-W ACG-6B rf power supply, and a 3-kW MFJ-949E tuner was used for rf circuit impedance matching. Typically, the reflected rf power did not exceed 3–5% of the forward power. This allowed sustaining a stable, diffuse, and uniform transverse discharge in air, nitrogen, and N_2–He mixtures. Initiating and sustaining of the rf discharge did not require flow preionization by the dc discharge upstream.

For electron density measurements in the test section, two rectangular microwave waveguides, 2 × 1 cm across, are placed on both sides of the nozzle immediately downstream of the rf electrodes. The electron density in the plasma is determined from the relative attenuation of a 10-GHz microwave signal across the plasma. The average electron density in the plasma is inferred from these measurements using the following relation[29]:

$$n_e = \left(m_e c \varepsilon_0 / e^2\right) \nu_{\text{coll}} (\delta V / V_{\text{inc}})(1/d) \tag{1}$$

where ν_{coll} is the electron–neutral collision frequency,

$$\delta V / V_{\text{inc}} = (V_{\text{trans}} - V_{\text{inc}}) / V_{\text{inc}}$$

is the relative attenuation factor in terms of the forward power detector voltage proportional to the incident and the transmitted microwave power, and $d = 7.5$ mm is the average distance between the internal nozzle walls in the test section (that is, at the location of the waveguides). The microwave attenuation measurement apparatus is described in greater detail in Ref. 29.

For the shock modification studies reported here, an 8-mm-long, 40-deg full angle plastic cone is inserted into the supersonic ionized flow 5 mm downstream of the rf electrodes, as shown in Fig. 1. The model is glued to a metal sting embedded in a thin plastic brace located in the diffuser. The distance between the test section side walls at the model location exceeds the model base diameter by about a factor of 2.2. The model occupies about 6% of the test section cross-sectional area. With this system, the effect of the nonequilibrium plasma on the strength of the resultant shock attached to the nose of the wedge can be studied in detail, in a steady and well-controlled plasma environment. The objective of the experiments is to measure the oblique shock angle, under both rf plasma-on and rf plasma-off conditions. It had been reported that the effect of the plasma is to weaken the shock. This should produce an apparent reduction of the shock Mach number and, therefore, increase the shock angle. Flow images visualized by the dc plasma were taken using a high-resolution monochrome camera COHU-4910.

III. Results and Discussion

The present experiments have been conducted in pure nitrogen, as well as in two different N_2–He gas mixtures, 70% N_2–30% He and 30% N_2–70% He, at the same plenum pressure of $P_0 = 250$ torr. At these conditions, the mass flow rate through the nozzle varies from 4.3 g/s in a 70% He mixture to 5.1 g/s in nitrogen. Both the axial dc and the transverse rf discharges were equally diffuse and stable in all gas mixtures used. The results of the dc and the rf current and voltage measurements at these conditions are summarized in Table 1. It can be seen that a sizable fraction of the dc power generated by the power supply is dissipated in the ballast resistor (from 25% in nitrogen up to 60% in a 30% N_2–70% He mixture). The reduced electric field in the aerodynamically stabilized dc discharge, determined from the measured dc voltage, plenum pressure, and the interelectrode distance varied in the range $(E/N)_{\text{dc}} = (4\text{–}6) \times 10^{-16}$ V · cm^2. At these conditions, up to 90% of the input electrical power goes to vibrational excitation of N_2 by electron impact rather than to direct gas heating.[28] This limits the maximum temperature rise in the dc discharge to only a few degrees. Indeed, for a nitrogen flow with a mass flow rate of 5.1 g/s and the dc discharge power of 290 W, the temperature rise can be estimated as $\Delta T \sim 5$ K. Because of the very slow rate of N_2 vibrational relaxation at these temperatures,[30] its contribution to the gas heating in the supersonic expansion flow is negligible.

Table 1 Discharge parameters: dc and rf

Run	U_{dc}, kV	I_{dc}, mA	dc power to plasma, W	rf power, W	U_{rf}, kV (rms)	I_{rf}, mA (rms)
			Gas mixture, 30% N_2–70% He			
1	17.0	25.2	175	100	0.78	72
2				200	1.28	111
3				250	1.42	119
			Gas mixture, 70% N_2–30% He			
4	20.0	17.3	225	200	1.28	130
5				300	1.70	176
6				350	1.84	184
			Gas, N_2			
7	25.0	15.3	290	200	1.28	122
8				300	1.70	173

Table 2 Electron density measurements

Run	dc power, W	rf power, W	$\delta V/V$	n_e, cm^{-3}
		Gas, N_2		
9	0	100	0.098	1.93×10^{11}
10		150	0.079	1.55×10^{11}
11		200	0.076	1.49×10^{11}
12		250	0.077	1.51×10^{11}
		Gas mixture, 70% N_2–30% He		
13		200	0.096	1.60×10^{11}
		Gas mixture, 30% N_2–70% He		
14		200	0.29	3.60×10^{11}
15	175	0	$<2.5 \times 10^{-3}$	$<3 \times 10^{9}$

The estimated reduced electric field based on the measured rms rf voltage and a distance between the rf electrodes of ~10 mm is significantly higher, $(E/N)_{rf} = (10\text{–}20) \times 10^{-16}$ V·cm^2. This estimate does not take into account the voltage drops across the quartz layers covering the electrodes, as well as across the plasma sheaths. The measured rms rf current varies from 72 to 184 mA, which gives the current density in the transverse rf discharge of $j = 100$–270 mA/cm^2. Although at these conditions a much smaller fraction of the input power goes to vibrational excitation,[28] the temperature rise in the rf discharge remains rather modest. Previous measurements[18] show that the temperature rise in the inviscid core of an $M = 2$, 30% N_2–70% He flow excited by a 200-W rf discharge is only $\Delta T = 15$ K.

The results of the electron density measurements are summarized in Table 2. The electron–neutral collision frequency required for the electron density inference ν_{coll} was obtained from the Boltzmann equation solution at $E/N = 10 \times 10^{-16}$ V·cm^2 (Ref. 31) using the experimental cross sections of elastic and inelastic electron–molecule collision processes available in the literature. At $P = 20$ torr and $T = 150$ K, the collision frequencies in pure nitrogen, 70% N_2–30% He mixture, and 30% N_2–70% He mixtures are $\nu_{coll} = 1.74 \times 10^{11}$ s^{-1}, 1.47×10^{11} s^{-1}, and 1.10×10^{11} s^{-1}, respectively. Note that the electron density in the rf discharge in pure nitrogen is nearly independent of the rf power (within ~25%), $n_e \cong (1.5\text{–}2.0) \times 10^{11}$ cm^{-3}. The observed electric current increase with the applied rf power (Table 1) is likely due to the electron drift velocity increase at a higher E/N. Increasing the helium partial pressure in the gas mixture up to 70% resulted in an electron density rise of about a factor of two, up to $n_e = 3.6 \times 10^{11}$ cm^{-3}. These values of electron density correspond to test section ionization fractions of $n_e/N = (1.2\text{–}3.0) \times 10^{-7}$, which are in the same range as the estimated ionization fractions in previous plasma shock experiments.[1,2,12,13]

In contrast, the test section electron density produced by the dc discharge afterglow in the nozzle plenum (with the rf discharge off) is much lower, $n_e < 3 \times 10^9$ cm^{-3}. In fact, in this case microwave absorption measurements did not show detectable absorption above the noise level. This dramatic difference between the electron densities in the dc discharge afterglow and in the rf discharge is mainly due to two factors: 1) the lower reduced electric field in the dc discharge and 2) the flow expansion between the nozzle plenum and the test section. Basically, the value of E/N in nonequilibrium discharges in molecular gases controls the electron energy balance. (For example, see Fig. 2 and Ref. 32.) An increase of E/N reduces the fraction of input power going into vibrational excitation and greatly increases the rates of both molecular dissociation and ionization (Fig. 2). This is consistent with previous measurements of the CO vibrational temperature in supersonic plasma flows sustained by dc and rf discharges.[18] Higher values of E/N in the transverse rf discharge are responsible for a higher electron impact ionization rate and, therefore, higher electron density. In addition, expansion of the dc afterglow plasma downstream of the nozzle throat reduces both the number density and the electron density in the test section. Note that the flow residence time in the nozzle, $\tau_{flow} \sim u/L \sim 50\text{–}100\ \mu$s, is too short to allow significant electron–ion recombination downstream of the dc discharge. (The recombination time is $\tau_{rec} \sim 1/\beta n_e \sim 1$ ms.) Here $u \sim 500\text{–}1000$ m/s is the flow velocity, $L \sim 5$ cm is the nozzle length, $\beta \sim 10^{-7}$ cm^3/s is the dissociative recombination rate, and $n_e \sim 10^{10}$ cm^{-3} is the electron density in the dc discharge estimated from the measured dc voltage and current.[17] This result suggests that a transverse rf discharge can be efficiently used to produce rather high electron densities, as well as atomic species and radical concentrations in supersonic flows of molecular gases.

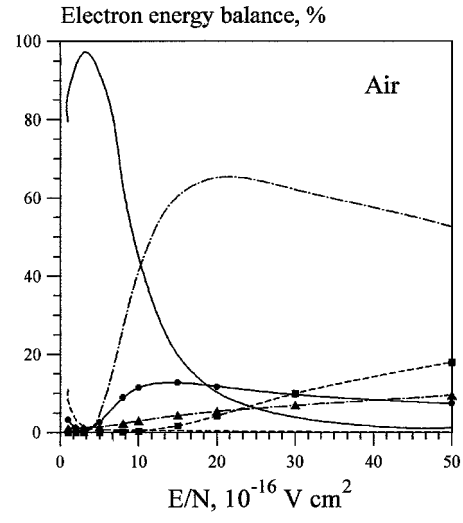

Fig. 2 Electron energy balance in air plasmas[32]: ——, vibrational excitation, N_2; – – –, vibrational excitation, O_2; –. –. –., electrical excitation, N_2; ●, electrical excitation, O_2; ■, ionization; and ▲, dissociation attachment to O_2.

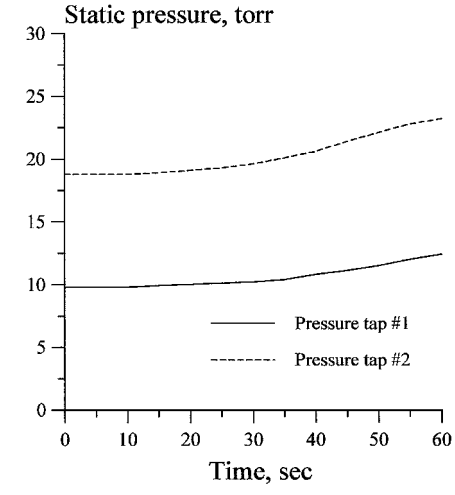

Fig. 3 Results of test section static pressure measurements, air at P_0 = 250 torr.

Figure 3 shows the results of the test section pressure measurements during the wind-tunnel operation with both dc and rf discharges turned off. Note that the static pressure remains stable and nearly constant (within 5%) for about 30 s before the back pressure starts rising. Turning the dc discharge on had almost no effect on the

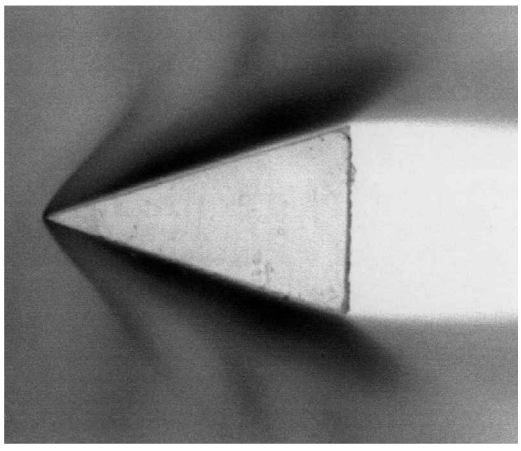

a)

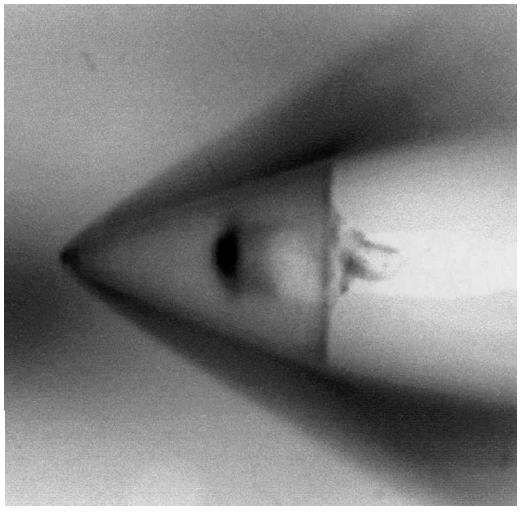

b)

Fig. 4 Inverted photographs of the supersonic flows visualized by the plasma generated by a dc discharge in the nozzle plenum at $P_0 = 250$ torr: a) 50% N_2–50% He flow over a 35-deg wedge[18] [the shock angle is 100 deg ($M = 2.05$)] and b) 30% N_2–70% He flow over a 40-deg cone [the shock angle is 69 deg ($M = 2.39$)].

test section pressure, whereas turning the rf discharge on resulted only in a slight pressure increase (within 1–3% depending on the rf power).

As in previous experiments,[18] with the dc and/or rf discharge on, the nozzle and the test section are filled with bright visible emission, arising primarily from the well-known second positive bands of nitrogen, $C^3\Pi_u \rightarrow B^3\Sigma_g$. This emission allows straightforward supersonic plasma flow and shock visualization.[17,18] As a first-order approximation, neglecting kinetic processes of population and decay of electronically excited radiating species, we can assume that the observed emission intensity, that is, the radiating species concentration, is simply proportional to the local number density. The rationale for this assumption is that the excited electronic level populations of N_2 are strongly coupled with the ground state vibrational populations of nitrogen, which relax extremely slowly. For example, the vibration–translation relaxation time of N_2 by He at the conditions of the present experiment is of the order of seconds,[31] whereas the flow residence time in the test section is of the order of tens of microseconds.

Figure 4 shows inverted black and white photographs of a supersonic N_2–He flow over a wedge in a quasi-two-dimensional plane nozzle[18] and a supersonic N_2–He flow over a cone in the nozzle shown in Fig. 1. Both flows are visualized by a dc discharge sustained in the nozzle plenum. Comparison of these two images shows significant qualitative differences. Indeed, the supersonic flowfield over the wedge appears to be quite complicated. First, one can see that the visible oblique shock attached to the wedge nose extends only over about one-quarter of the wedge length. Second, there appears to be a fainter secondary shock formed about halfway along the wedge. Finally, there are two distinct bright features formed near the wedge surface that look similar to boundary layers. On the other hand, the supersonic flow over the cone appears to be much less complicated. The entire region behind the shock is filled with bright, nearly uniform visible emission, with no apparent bright or dark structures (Fig. 4). This observation is consistent with our assumption regarding the correlation between the emission intensity and the local number density. Indeed, in the absence of the shock perturbation by the nozzle walls, the number density of the flow behind the conical shock is expected to be uniform. The conical shock front looks somewhat less distinct compared to the oblique shock front (Fig. 4) because in the former case we are looking at a three-dimensional object that is not entirely in focus.

This qualitative analysis suggests that the flow over a wedge in the quasi-two-dimensional plane nozzle studied in previous experiments[17,18] is rather strongly perturbed by the nozzle side walls, which were only 4–5 mm apart. In the wedge flow shown in Fig. 4a, the oblique shock angle of $\alpha = 100$ deg indicates a test section Mach number of $M = 2.05$. In the cone flow, the shock angle is $\alpha = 68$ deg, which corresponds to a Mach number of $M = 2.39$. The shock angle is measured with an accuracy of ± 0.75 deg, which was found by comparing the angle determined from several frames of a high-resolution video camera taken during the same run at a rate of about 1 frame per second.

Unlike previous experiments,[18] turning the rf discharge on and off during the wind-tunnel operation did not result in a detectable

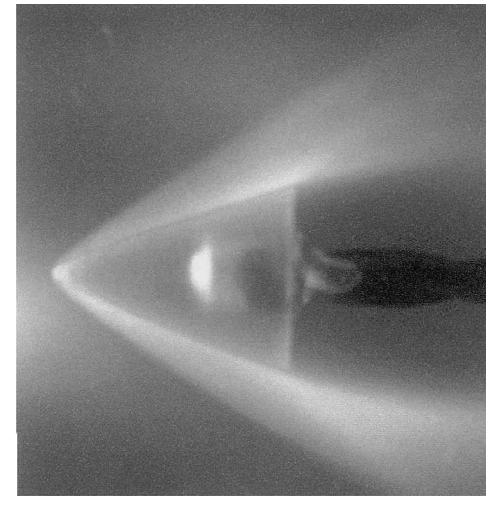

a)

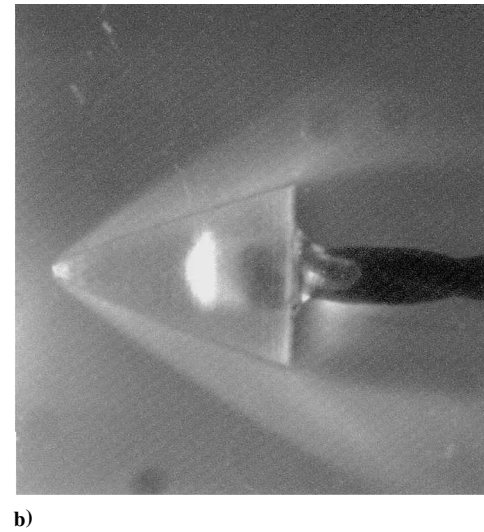

b)

Fig. 5 Photographs of the supersonic flow over a cone visualized by the plasma generated by a dc and an rf discharges in a 30% N_2–70% He flow at $P_0 = 250$ torr: a) only the 175-W dc discharge is on and b) both the 175-W dc and the 250-W rf discharge are on.

shock angle increase. These measurements have been done in all three gas mixtures considered. In these measurements, the dc discharge remained on all of the time to provide plasma flow visualization and enable shock angle measurements with the rf discharge off. The maximum rf discharge power applied was 350 W. This is almost twice the maximum rf power used in previous experiments in a quasi-two-dimensional plane nozzle (200 W) (Ref. 18), which resulted in a considerable shock weakening. As an example, Fig. 5 shows two typical flow images obtained in a 30% N_2–70% He flow over a cone with the 250-W rf discharge turned on and off. In all runs, the shock angle with the rf discharge turned on was within about 1 deg from its value with the rf discharge turned off, $\alpha = 68$ deg. At all experimental conditions, the shock front appeared sharp and well defined, with no evidence of splitting or dispersion (Fig. 5).

In previous shock weakening experiments in a supersonic flow over a 35-deg wedge,[18] the oblique shock angle in a 30% N_2–70% He flow increased from $\alpha = 99$ deg to $\alpha' = 113$ deg, which corresponds to an apparent Mach number reduction from $M = 2.06$ to $M' = 1.88$ ($M'/M \cong 0.913$). In a supersonic flow over a cone, the shock angle change that corresponds to such Mach number reduction, from $M = 2.39$ to $M' = 2.18$, is substantially smaller because of the three-dimensional relief effect, from $\alpha = 68$ deg to $\alpha' = 72$ deg. However, a 4-deg angle change considerably exceeds the accuracy of the present shock angle measurements, and a consistent shock angle increase of such magnitude would certainly have been detected.

IV. Conclusions

Removal of the heated boundary layers, which contributed to the shock weakening in previous plasma wind-tunnel experiments,[18] as well as the resulting reduction of gas temperature gradients in the supersonic test section, essentially resulted in disappearance of the effect of the plasma on the shock strength. Although in the present experiments the rf discharge power substantially exceeded the power used in previous work,[18] this did not produce any detectable shock weakening. Therefore, we conclude that the heated boundary-layer/oblique shock interaction was indeed the only reason for the previously reported shock weakening in the plasma wind tunnel. Also, because in the present experiments both the flow and the plasma parameters [$P = 10$–20 torr, $M = 2.4$, and $n_e/N = (1.2$–$3.0) \times 10^{-7}$] are comparable with their values in previous plasma shock experiments,[1,2,12,13] the present results strongly suggest that previously reported anomalous shock behavior in nonequilibrium plasmas is due to thermal effects alone.

Acknowledgments

Support from the Air Force Office of Scientific Research (Grant 49620-99-1-0023) is gratefully acknowledged. We also thank S. Merriman, B. Kowalczyk, and A. Christian for their help with the design of the supersonic test section.

References

[1]Klimov, A. I., Koblov, A. N., Mishin, G. I., Serov, Y. L., and Yavor, I. P., "Shock Wave Propagation in a Glow Discharge," *Soviet Technical Physics Letters*, Vol. 8, No. 4, 1982, pp. 192–194.

[2]Klimov, A. I., Koblov, A. N., Mishin, G. I., Serov, Y. L., Khodataev, K. V., and Yavor, I. P., "Shock Wave Propagation in a Decaying Plasma," *Soviet Technical Physics Letters*, Vol. 8, No. 5, 1982, pp. 240–241.

[3]Basargin, I. V., and Mishin, G. I., "Probe Studies of Shock Waves in the Plasma of a Transverse Glow Discharge," *Soviet Technical Physics Letters*, Vol. 11, No. 11, 1985, pp. 535–538.

[4]Gorshkov, V. A., Klimov, A. I., Mishin, G. I., Fedotov, A. B., and Yavor, I. P., "Behavior of Electron Density in a Weakly Ionized Nonequilibrium Plasma with a Propagating Shock Wave," *Soviet Physics—Technical Physics*, Vol. 32, No. 10, 1987, pp. 1138–1141.

[5]Ershov, A. P., Klishin, S. V., Kuzovnikov, A. A., Ponomareva, S. E., and Pyt'ev, Y. P., "Application of the Reduction Method to the Microwave Interferometry of Shock Waves in Weakly Ionized Plasma," *Soviet Physics—Techical Physics*, Vol. 34, No. 8, 1989, pp. 936–937.

[6]Basargin, I. V., and Mishin, G. I., "Precursor of Shock Wave in Glow-Discharge Plasma," *Soviet Technical Physics Letters*, Vol. 15, No. 4, 1989, pp. 311–313.

[7]Bystrov, S. A., Zaslonko, I. S., Mukoseev, Y. K., and Shugaev, F. V., "Precursor Ahead of a Shock Front in an RF Discharge Plasma," *Soviet Physics—Doklady*, Vol. 35, No. 1, 1990, pp. 39, 40.

[8]Mishin, G. I., Serov, Y. L., and Yavor, I. P., "Flow Around a Sphere Moving Supersonically in a Glow Discharge Plasma," *Soviet Technical Physics Letters*, Vol. 17, No. 6, 1991, pp. 413–416.

[9]Mishin, G. I., Klimov, A. I., and Gridin, A. Y., "Measurements of the Pressure and Density in Shock Waves in a Gas Discharge Plasma," *Soviet Technical Physics Letters*, Vol. 17, No. 8, 1992, pp. 602–604.

[10]Gridin, A. Y., Klimov, A. I., and Khodataev, K. V., "Propagation of Shock Waves in a Nonuniform Transverse Pulsed Discharge," *High Temperature*, Vol. 32, No. 4, 1994, pp. 454–457.

[11]Bedin, A. P., and Mishin, G. I., "Ballistic Studies of the Aerodynamic Drag on a Sphere in Ionized Air," *Technical Physics Letters*, Vol. 21, No. 1, 1995, pp. 5–7.

[12]Ganguly, B. N., Bletzinger, P., and Grascadden, A., "Shock Wave Dispersion in Nonequilibrium Plasmas," *Physics Letters A*, Vol. 230, No. 3–4, 1997, pp. 218–222.

[13]Bletzinger, P., and Ganguly, B. N., "Local Acoustic Shock Velocity and Shock Structure Recovery Measurements in Glow Discharges," *Physics Letters A*, Vol. 258, No. 4–6, 1999, pp. 342–348.

[14]Lowry, H., Smith, M., Sherrouse, P., Felderman, J., Drakes, J., Bauer, M., Pruitt, D., and Keefer, D., "Ballistic Range Tests in Weakly Ionized Argon," AIAA Paper 99-4822, June–July 1999.

[15]Lowry, H., Stepanek, C., Crosswy, L., Sherrouse, P., Smith, M., Price, L., Ruyten, W., and Felderman, J., "Shock Structure on a Spherical Projectile in Weakly Ionized Air," AIAA Paper 99-0600, Jan. 1999.

[16]Ionikh, Y. Z., Chernysheva, N. V., Meshchanov, A. V., Yalin, A. P., and Miles, R. B., "Direct Evidence for Thermal Mechanism of Plasma Influence on Shock Wave Propagation," *Physics Letters A*, Vol. 259, No. 5, 1999, pp. 387–392.

[17]Yano, R., Contini, V., Plönjes, E., Palm, P., Merriman, S., Aithal, S., Adamovich, I., Lempert, W., Subramaniam, V., and Rich, J. W., "Supersonic Nonequilibrium Plasma Wind Tunnel Measurements of Shock Modification and Flow Visualization," *AIAA Journal*, Vol. 38, No. 10, 2000, pp. 1879–1888.

[18]Merriman, S., Plönjes, E., Palm, P., and Adamovich, I. V., "Shock Wave Control by Nonequilibrium Plasmas in Cold Supersonic Gas Flows," *AIAA Journal*, Vol. 39, No. 8, 2001, pp. 1547–1552.

[19]White, A. R., and Subramaniam, V. V., "Shock Propagation Through a Low-Pressure Glow Discharge in Argon," *Journal of Thermophysics and Heat Transfer*, Vol. 15, No. 4, 2001, pp. 491–496.

[20]Avramenko, R. F., Rukhadze, A. A., and Teselkin, S. F., "Structure of a Shock Wave in a Weakly Ionized Nonisothermal Plasma," *Soviet Physics—JETP Letters*, Vol. 34, No. 9, 1981, pp. 463–466.

[21]Vstovskii, G. V., and Kozlov, G. I., "Propagation of Weak Shock Waves in a Vibrationally Excited Gas," *Soviet Technical Physics*, Vol. 31, No. 8, 1986, pp. 911–914.

[22]Soloviev, V., Krivtsov, V., Konchakov, A., and Malmuth, N. D., "Mechanisms of Shock Wave Dispersion and Attenuation in Weakly Ionized Cold Discharge Plasmas," AIAA Paper 99-4908, June–July 1999.

[23]Bychkov, V., and Malmuth, N. D., "Shock Wave Structure in Nonequilibrium Ar Discharge Plasma," AIAA Paper 99-4938, June–July 1999.

[24]Bailey, W. F., and Hilbun, W. M., "Baseline of Thermal Effects on Shock Propagation in Glow Discharges," *Proceedings of Workshop on Weakly Ionized Gases*, U.S. Air Force Academy, Colorado Springs, CO, 1997, pp. GG3–GG18.

[25]Macheret, S. O., Ionikh, Y. Z., Chernysheva, N. V., Yalin, A. P., Martinelli, L., and Miles, R. B., "Shock Wave Propagation and Dispersion in Glow Discharge Plasmas," *Physics of Fluids*, Vol. 13, No. 9, 2001, pp. 2693–2705.

[26]Aithal, S., and Subramaniam, V. V., "On the Characteristics of a Spark Generated Shock Wave," *Physics of Fluids*, Vol. 12, No. 4, 2000, pp. 924–934.

[27]Adamovich, I. V., Subramaniam, V. V., Rich, J. W., and Macheret, S. O., "Phenomenological Analysis of Shock Wave Propagation in Weakly Ionized Plasmas," *AIAA Journal*, Vol. 36, No. 5, 1998, pp. 816–822.

[28]Raizer, Yu. P., *Gas Discharge Physics*, Springer, Berlin, 1991, Chap. 5.

[29]Palm, P., Plönjes, E., Buoni, M., Subramaniam, V. V., and Adamovich, I. V., "Electron Density and Recombination Rate Measurements in CO-Seeded Optically Pumped Plasmas," *Journal of Applied Physics*, Vol. 89, No. 11, 2001, pp. 5903–5910.

[30]Billing, G. D., "Vibration–Vibration and Vibration–Translation Energy Transfer, Including Multiquantum Transitions in Atom–Diatom and Diatom–Diatom Collisions," *Nonequilibrium Vibrational Kinetics*, Springer-Verlag, Berlin, 1986, Chap. 4, pp. 85–111.

[31]Adamovich, I. V., and Rich, J. W., "The Effect of Superelastic Electron–Molecule Collisions on the Vibrational Energy Distribution Function," *Journal of Physics D: Applied Physics*, Vol. 30, No. 12, 1997, pp. 1741–1745.

[32]Aleksandrov, N. L., Vysikailo, F. I., Islamov, R. S., Kochetov, I. V., Napartovich, A. P., and Pevgov, V. G., "Electron Distribution Function in a N_2:O_2 = 4:1 Mixture," *Soviet High Temperature*, Vol. 19, No. 1, 1981, pp. 22–29.

M. Sichel
Associate Editor